

## Characterization of surface heterogeneity detected at the MISR/TERRA subpixel scale.

Jean-Luc Widlowski, Bernard Pinty, Nadine Gobron, Michel M. Verstraete  
GVM Unit, Space Applications Institute, Joint Research Centre, TP 440, Ispra I-21020 (VA), Italy

Anthony B. Davis

Los Alamos National Laboratory, Space and Remote Sensing Group, Los Alamos, NM 87545, USA

**Abstract.** Vegetation structure can have a significant impact on the degree of anisotropy in the reflected radiation field. With the appropriate characterization of these effects, the analysis of multiangular data, such as provided by the Multi-angle Imaging SpectroRadiometer (MISR) instrument on board TERRA, can yield statistical information about the type of surface heterogeneity that exists at the subpixel scale.

### Introduction

Retrieving information about the state of terrestrial vegetation canopies has typically been restricted to the scale of individual pixels, that is, instantaneous (multi) spectral measurements are treated as if the signal contributing surfaces were composed of a single uniformly distributed cover type. To address the issue of subpixel variability, approaches like the independent pixel approximation (IPA), linearly combine the spectral reflectances of two or more homogeneous end-members [*e.g.*, Cahalan *et al.* 1994]. However, in order to account explicitly for the architecture of spatially heterogeneous vegetation canopies, three-dimensional radiation transfer models need to be employed in the retrieval strategy, [*e.g.*, Widlowski *et al.* 2001]. This may deliver realistic canopy architecture representations of the potential surface types, but such approaches are generally computationally-intensive and have yet to provide a means of characterizing the spatial structure of the retrieved vegetation types. Pinty *et al.* [2000] recently showed that the analysis of multi-angular reflectance data in the red spectral domain may yield information about the heterogeneity of the surface at the sensor subpixel scale. This approach is exploited by Gobron *et al.* [2001] to retrieve information on vegetation activity and structure from the Multi-angle Imaging SpectroRadiometer (MISR) instrument [Diner *et al.*, 1998] on board EOS-TERRA. In the present work, this radiatively derived surface heterogeneity indicator  $k$  will be related to actual vegetation canopy height fields as characterized by their first-order structure-function [Mandelbrot, 1982] and singularity measure [Hentschel and Procaccia, 1983] exponents. Although the latter have been amply used in the context of multifractal cloud and rain characterizations, [*e.g.*, Lovejoy and Schertzer 1990], this paper utilizes

these statistical indicators solely as tools for pursuing new avenues in understanding how vegetation structure affects the reflectance anisotropy that can be measured by the latest generation of multi-directional instruments, like MISR.

### Canopy Height Field Characterization

Other than topography and the leaf and soil optical properties, the abundance, dimensions and spatial aggregations of dominant vegetation types within the footprint area of a space-borne sensor are the primary modulators of the angular anisotropy in the surface-leaving reflectance field, especially in the red spectral domain. Canopy height measurements may provide a convenient way to quantify the degree of spatial heterogeneity within the field of view of an observing instrument. However, several of the techniques to analyze such data transects, like the auto-correlation and statistical moment analysis, become meaningless if the signal does not exhibit spatial *stationarity*, that is, invariance of statistical properties under translation [Davis *et al.*, 1994]. Others, like Fourier spectrum slopes and semi-variograms may suffer from what has been termed the *ambiguity* of data sets, *i.e.*, very different looking geophysical signals may exhibit identical statistics. Davis *et al.* [1994] have argued that the first order structure function exponent  $H_1$  proves sufficient to quantify the non-stationarity of any generic geophysical signal  $\phi(x)$ :

$$\langle |\phi(x+r) - \phi(x)| \rangle \propto \left(\frac{r}{L}\right)^{H_1} \quad (\ell \leq r \leq L) \quad (1)$$

where  $\ell$  is the sampling interval of  $\phi(x)$  along the segment  $[0, L]$ , and  $\langle \cdot \rangle$  indicates ensemble averaging over the scale  $r$  within the length of the data set  $L$ . Bound in the range  $[0, 1]$ ,  $H_1$  allows for an intuitive geometric interpretation of the signal under study: Low values relate to increased roughness (more stationarity) in the data set whereas high values indicate the presence of smoothness (more non-stationarity).

However, like the fractal dimension,  $H_1$  becomes an ambiguous descriptor of the variability in the case of multi-affine signals. In order to remove this indetermination Davis *et al.*, [1994] proposed to additionally characterize the role of *intermittency* in the observed signal. This can be achieved using different flavors of ‘singularity analysis’ to define a hierarchy of exponents from which the intermittency descriptor  $C_1$  can be derived [Schertzer and Lovejoy, 1987]. Like  $H_1$ ,  $C_1$  is confined to the range  $[0, 1]$ . At  $C_1 = 0$  the data exhibit no intermittency but similar variability everywhere (*e.g.*, Gaussian processes), whereas  $C_1 = 1$  relates to highly singular occurrences of variability (*e.g.*, random Dirac delta

Copyright 2001 by the American Geophysical Union.

Paper number 2001GL013490.  
0094-8276/01/2001GL013490\$05.00

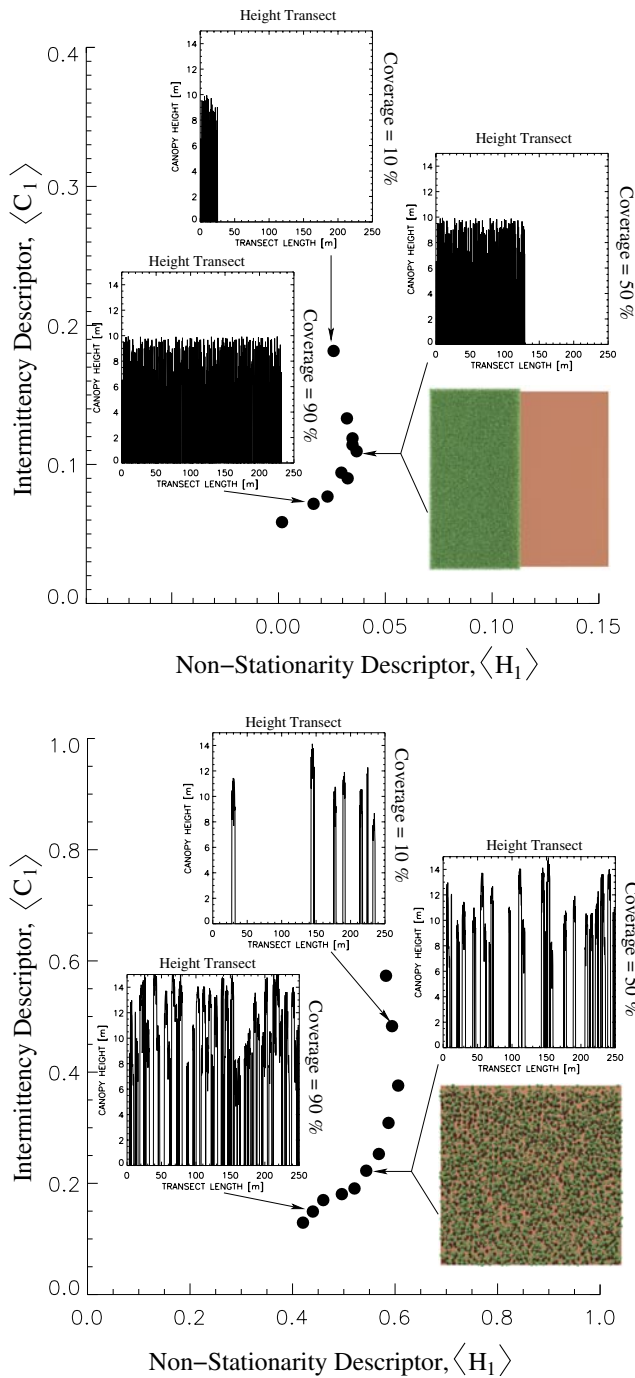


**Figure 1.**  $\langle H_1 \rangle, \langle C_1 \rangle$  statistics for various canopies of different vegetation coverage. The top (bottom) panel refers to radiatively homogeneous (heterogeneous) vegetation canopies. Typical height transects of the low (10%), medium (50%) and high (90%) vegetation covers as well as a graphical representation of the intermediate cases are presented.

functions). In the latter, extremely intermittent case, the occurrence of dominant signal variations may be characterized as being ‘sparse’ whereas in the former case it is ‘dense’. Analyzing  $H_1$  and  $C_1$  has proven useful in a variety of geographical situations, [e.g., Marshak et al. 1997].

To gather the necessary canopy height data, the model of Govaerts and Verstraete [1998] was used to generate various 3-D vegetation canopy representations at the nominal

ground resolution of the MISR instrument. The sampling interval of the subsequent height measurements ( $\ell \simeq 25$  cm), was chosen such as to be greater than the characteristic scale of the leaves, yet smaller than the typical dimension of the tree crowns or the gaps in between them. 40 transects of equal length ( $2^{10}$  data points) but with different origins and orientations were sampled. For each of these, the  $H_1$ ,  $C_1$  statistics were computed in the small scale limit following the approach of Davis et al., [1994]. The structure functions were fitted (on a log-log plot) from scale  $\eta = \ell$  to the first detected scale break ( $\sim 1$ –2 orders of magnitude), or, in its absence, through all the data.  $C_1$  was computed from a normalized absolute gradient field of step size  $\eta$ . Ultimately, these  $H_1$ ,  $C_1$  statistics were ensemble averaged to yield a directionally independent estimate of the non-stationarity  $\langle H_1 \rangle$  and intermittency  $\langle C_1 \rangle$  of the vegetation height at the resolution of the MISR pixel (275 m). Tests have indicated that the actual values of these ensemble averaged statistics vary, from  $\sim 0.02$  at high values to  $\sim 0.05$  at low values of vegetation coverage, if different sets of transects were selected.

In the context of this paper, radiatively homogeneous canopies refer to surface conditions where the bidirectional reflectance factor (BRF) fields produced by plane-parallel radiative transfer (RT) models (together with the IPA) are indiscernible from those generated by a full 3-D RT models. Thus, in Figure 1, the  $\langle H_1 \rangle$ ,  $\langle C_1 \rangle$  statistics for radiatively homogeneous (top) and heterogeneous (bottom) vegetation canopies are shown. Typical height transects of the low, medium and high vegetation coverages as well as a graphical representation of the intermediate case are presented. For the documented simulations intermittency naturally decreases with increasing vegetation cover. Non-stationarity,

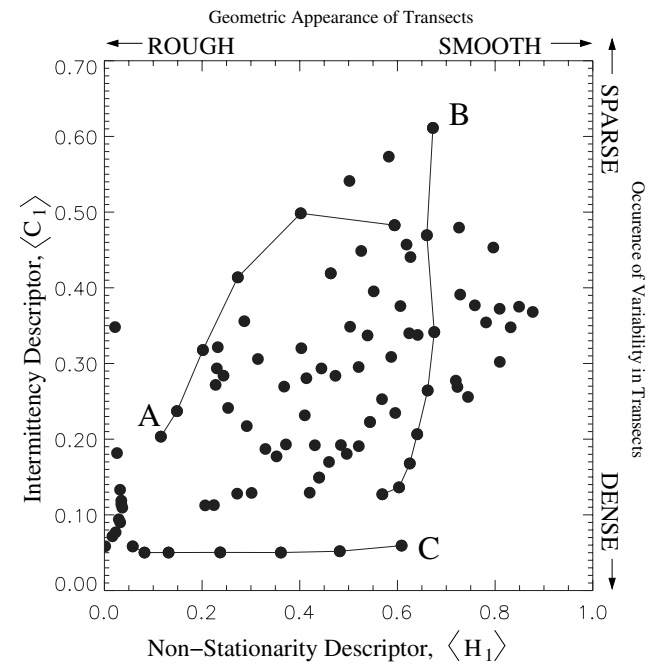


**Figure 2.**  $\langle H_1 \rangle, \langle C_1 \rangle$  statistics for a large variety of different vegetation canopies, e.g., **A**: low density deciduous forest of increasing coverage (left to right), **B**: boreal forest of increasing stand density (top to bottom), **C**: closed rainforest of decreasing canopy depth (left to right) and equal leaf content.

on the other hand, tends to be highest at low to medium vegetation coverages, decreasing at very low coverages due to most transects showing only a few jumps, and also at very high coverages because here stationarity is asymptotically approached (*i.e.*, height-transects and white-noise graphs start looking alike). For radiatively homogeneous vegetation canopies the non-stationarity and intermittency descriptors are remarkably lower than for their heterogeneous counterparts. These findings suggest the ability of  $\langle H_1 \rangle$ ,  $\langle C_1 \rangle$  to characterize different vegetation structures through their corresponding canopy height fields. Figure 2 corroborates this by documenting the differing intermittency and non-stationarity behaviors of such diverse biome types as **A**, low density deciduous forest of increasing coverage (left to right), **B**, evergreen boreal forest of increasing stand density (top to bottom) and **C**, closed rainforest of equal leaf content and decreasing canopy depth (left to right), for example [Widlowski *et al.*, 2001].

## Combining Canopy Height Field and Reflectance Anisotropy Descriptors

The angular anisotropy of a surface exiting radiation field in the optical domain can be partly qualified with the Minnaert function parameter,  $k$ , of the RPV model [Pinty *et al.*, 2000]. If sufficient spectral contrast exists between the (darker) canopy foliage and the underlying (brighter) ground cover, different types of vegetation structure yield different BRDF fields. Figure 3 shows typical examples of homogeneous (left) and heterogeneous (right) vegetation canopy BRDFs in the cross plane. The reflectance field of homogeneous canopies can either be generated using explicit 3-D RT models or equivalently by combining the radiances generated with 1-D plane-parallel RT models using the IPA approach. These BRDFs may be characterized by a *bowl-shape* and  $k$  values less than 1. For heterogeneous canopies, where the visible (relatively bright) soil fraction decreases from nadir to oblique viewing angles, the corresponding BRDF shapes may be *bell-shape* in which case the  $k$  value is greater than 1. The latter obviously depends on the foliage orientation, distribution and density, the optical properties of both the leaves and the ground, as well as the illumination angle and the field of view of the sensor.

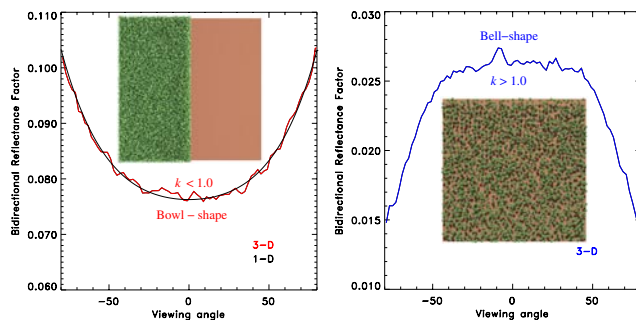


**Figure 3.** Typical BRDF anisotropy in the red spectral domain for radiatively homogeneous (left) and heterogeneous (right) vegetation canopies. The BRDFs of the heterogeneous surface are generated using a 3-D RT model and typified by a bell-shape ( $k > 1$ ). The BRDFs of the homogeneous surface covers are generated using a 3D RT model and a 1D IPA approach, and are generally bowl-shaped ( $k < 1$ ).

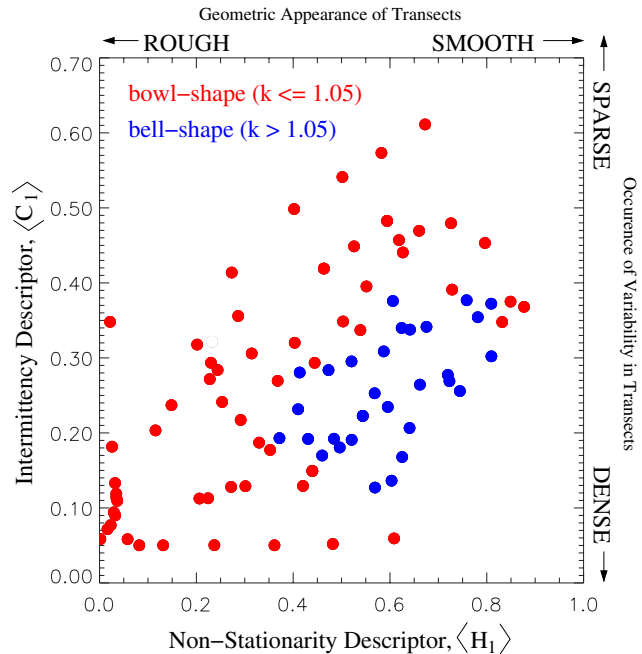


**Figure 4.**  $\langle H_1 \rangle, \langle C_1 \rangle$  statistics for a large variety of different vegetation canopies overlaid by their corresponding reflectance anisotropy quantifier,  $k$ . Shown in red (blue) are all canopy types that generate bowl-shaped (bell-shaped) reflectance fields *e.g.*,  $k \leq 1.05$  ( $k > 1.05$ ).

Simulating the reflectance fields in the red band and at the nominal ground resolution of MISR allows one to retrieve the radiative anisotropy quantifier  $k$  for all of the vegetation types characterized in Figure 2. The BRDF modelling was performed with the Raytran model of Govaerts and Verstraete [1998] for a solar zenith angle of  $30^\circ$ , uniform leaf angle distributions, Lambertian scattering properties of both soil and leaves, and leaf reflectance (transmittance) values of 0.055 (0.015) and 0.127 for the soil albedo. In Figure 4, the value of  $k$  was discriminated with colour against the corresponding  $\langle H_1 \rangle$ ,  $\langle C_1 \rangle$  statistics. Shown in red (blue) are all canopy types that generate bowl-shaped (bell-shaped) reflectance fields with  $k \leq 1.05$  ( $k > 1.05$ ). Given the simulated conditions a remarkable pattern of organisation can be observed: only the presence of vertically elongated foliage clumps (tree crowns) of medium to high densities can generate bell shaped BRDF fields. Sparse tree coverage and closed vegetation canopies, on the other hand, will have a value of  $k$  that is generally less than 1. Thus, based on spectral signatures and the retrieved values of  $k$  [Gobron *et al.*, 2001], it is envisaged that the vegetation structure at the sub-pixel scale of the observing instrument may be deduced (under appropriate sampling conditions) from a set of predefined  $\langle H_1 \rangle$ ,  $\langle C_1 \rangle$  statistics, corresponding to typical configurations of the most likely biome types to be encountered within the region of study.

## Conclusion

It has been shown that vegetation canopy structure may be characterized in the small scale limit by non-stationarity ( $\langle H_1 \rangle$ ) and intermittency ( $\langle C_1 \rangle$ ) exponents using an ensemble of canopy height transects of different orientations and origins. More importantly, the reflectance anisotropy

quantifier  $k$ , obtained by inversion of the parametric RPV model against multiangular terrestrial surface observations, when used in conjunction with the corresponding  $\langle H_1 \rangle$ ,  $\langle C_1 \rangle$  statistics, allows to identify specific types of vegetation that are characterized by medium-dense accumulations of vertically elongated foliage clumps. Therefore, if sufficient spectral contrast exists between the (darker) leaves and (brighter) ground cover in the red,  $k$  may be employed (in conjunction with spectral information and under appropriate sampling conditions) to characterize the underlying vegetation structure at the scale of the MISR subpixel resolution.

## References

- Cahalan, R., W. Ridgeway, and W. J. Wiscombe, Independent Pixel and Monte Carlo Estimates of Stratocumulus Albedo, *Journal of the Atmospheric Sciences*, 51, 3776–3790, 1994
- Davis, A., A. Marshak, W. Wiscombe, and R. Cahalan, Multifractal characterization of nonstationarity and intermittency in geophysical fields: Observed, retrieved, or simulated, *J. Geophys. Res.*, 99, 8055–8072, 1994
- Diner, D. J., J. C. Beckert, T. H. Reilly, C. J. Bruegge, J. E. Conel, R. Kahn, J. V. Martonchik, T. P. Ackerman, R. Davies, S. A. W. Gerstl, H. R. Gordon, J. P. Muller, R. B. Myneni, P. J. Sellers, B. Pinty, and M. M. Verstraete, Multiangle Imaging Spectroradiometer (MISR) description and experiment overview. *IEEE Transactions on Geoscience and Remote Sensing*, 36, 1072–1087, 1998.
- Gobron N., B. Pinty, J.-L. Widlowski, M. M. Verstraete and D. J. Diner, Joint Retrieval of Vegetation Structure and Photosynthetic Activity from MISR. *Proceedings of IGARSS 2001*, July 9-13, Sydney, Australia, 2001.
- Govaerts, Y., and M. M. Verstraete, Raytran: A Monte Carlo Ray Tracing Model to Compute Light Scattering in Three-Dimensional Heterogeneous Media, *IEEE Transactions on Geoscience and Remote Sensing*, 36, 493–505, 1998
- Hentschel, H. G. E., and I. Procaccia, The infinite number of generalized dimensions of fractals and strange attractors, *Physica D*, 8, 435–444, 1983.
- Lovejoy, S. and Schertzer, D., Fractals, raindrops and resolution dependence of rain measurements. *Journal of Applied Meteorology*, 29, 1167–1170, 1990
- Mandelbrot, B. B., *The Fractal Geometry of Nature*, 460 pp., W. H. Freeman, San Francisco (Ca), 1982.
- Marshak, A., A. Davis, W. Wiscombe, and R. Cahalan, Scale Invariance in Liquid Water Distributions in Marine Stratocumulus. Part II: Multifractal Properties and Intermittency Issues, *Journal of the Atmospheric Sciences*, 54, 1423–1444, 1997
- Pinty, B., J.-L. Widlowski, N. Gobron, M. M. Verstraete, and the MISR Team, Detection of Land Surface Structure and Heterogeneity from MISR/Terra Data. *Proceedings of the Fall Meeting of the American Geophysical Union*, December 15-19, San Francisco, California, Published as a supplement to EOS, Transactions, AGU, Vol 81, No 48, F275, 2000.
- Schertzer D. and S. Lovejoy, Physical modelling and analysis of rain and clouds by anisotropic scaling and multiplicative processes, *J. Geophys. Res.*, 92 (D8), 9693–9714, 1987
- Widlowski, J.-L., B. Pinty, N. Gobron, and M. M. Verstraete, Detection and characterization of boreal coniferous forests from remote sensing data, *J. Geophys. Res.*, 2001, in print
- 
- J.-L. Widlowski, B. Pinty, N. Gobron and M. M. Verstraete, Global Vegetation Monitoring Unit, Institute for Environment and Sustainability, Joint Research Centre, TP 440, Ispra I-21020 (VA), Italy. (e-mail: Jean-Luc.Widlowski@jrc.it; Bernard.Pinty@jrc.it; Nadine.Gobron@jrc.it; Michel.Verstraete@jrc.it)
- A. B. Davis, Los Alamos National Laboratory, Space and Remote Sensing Group, Los Alamos, NM 87545, USA. (e-mail: adavis@lanl.gov)

(Received May 22, 2001; revised August 27, 2001; accepted September 5, 2001.)